Multi-resolution decomposition in relation to characteristic scales and local window sizes using an operational wavelet algorithm

Soe W. Myint

Working Paper Number 2010-05

Multi-resolution decomposition in relation to characteristic scales and local window sizes using an operational wavelet algorithm

SOE W. MYINT

School of Geographical Sciences, Arizona State University

P.O. Box 870104, Tempe, AZ 85287-0104

Email: soe.myint@asu.edu

Phone: (480) 965-6514; Fax: (480) 965-8313

Abstract

Data from an IKONOS image acquired over Dallas was used to demonstrate the use of an operational wavelet-based algorithm to examine the performance of different texture measures and window sizes at various resolutions in connection to characteristic scales. It was found that a 63x63 window was the optimal window size, and energy measure produced the highest accuracy. Results from this study suggest that the choice of window size in wavelet-based classification affects the accuracy. Larger window sizes significantly improve the overall accuracy when using homogeneous samples. In the real-world situation, a larger window may not necessarily produce higher accuracy since a larger window tends to cover more land-use and land-cover classes and therefore may miss smaller regions of classes that could lead to poorer accuracy. On the other hand, a smaller window tends to be incomplete in its coverage of texture features that represent a complex class. The classification accuracy can be improved by using more combinations of sub-images at different scales. However, smaller sub-images at the last two levels may lower the classification accuracy. The characteristic scale of the most complex feature among all selected classes could be the optimal local window size necessary to achieve the highest accuracy.

Keywords: wavelets, land use land cover, local window, characteristic scale

1. Introduction

Despite the widespread availability, frequency of updates, fine spatial resolution, and cost efficiency of the recent generation of remotely sensed data (e.g., IKONOS from April 1999 - http://www.geoeye.com/products/imagery/ikonos/default.htm; QuickBird from October 2001 - http://www.digitalglobe.com/about/quickbird.html), the use of remote sensing technology for urban mapping still remains a challenging task. It is generally accepted that higher spatial resolution is more desirable than higher spectral resolution in urban mapping (Jensen and Cowen, 1999). However, with higher spatial resolution, spectral responses from smaller objects and features (e.g., rubber, plastic, shingle, metal, concrete, asphalt, wood, brick, soil, vegetation) become distinguishable. As a result, these high spatial resolution images over urban areas contain many edges and small objects, and appear complex and noisy, making the classification of urban land-covers (and subsequent inference of urban land-use classes) using the traditional per-pixel classification approaches (e.g., maximum likelihood classifier, Mahalanobis decision rule) difficult. There is a growing need for more accurate image processing techniques to analyze and classify these high-resolution data sets (Chen and Stow, 2003).

In land-use and land-cover classification, the objective is to identify a class that may be composed of many small objects and features but not any individual objects and features within that class (Campbell, 2002). In other words, we are interested in identifying the composite (e.g., residential, commercial) of different features and objects (e.g., cement roads, tar roads, houses, grasses, shrubs, trees, bare soil, driveways, swimming pools, parking lots, and sidewalks) rather than attempting to have a collection of those many small components that may be of little or no interest to researchers, policy makers, or planners for consequent analysis or planning and decision making.

In the study of pattern recognition and interpretation, one of the key elements that the human visual system uses to recognize most spatial objects is their texture (Bergen and Julesz,

1983). Even though human eyes can recognize complex patterns in images and distinguish between, for example, residential and commercial classes, the commonly used classification approaches that employ the original spectral bands encounter serious problems in identifying urban classes since they primarily use spectral information instead of the spatial association of surrounding objects and elements. This is because urban land-use classes generally show high variation in the spectral response of their component land-cover types (Foster, 1985; Gong and Howarth, 1990; Barnsley et al., 1991) and the training statistics of these classes exhibit very high standard deviation or variances (Sadler et al., 1991). The data distribution of these classes may also violate one of the important assumptions of the traditional statistical classifiers (e.g., Maximum likelihood decision rule) that the pixel values follow a normal distribution (Barnsley et al., 1991; Sadler et al., 1991). The classification accuracy of images is the result of a trade-off between two main issues: class boundary pixels and within-class variances (Metzger and Muller, 1996). Hence, the spectral per-pixel classification approaches (e.g., Maximum likelihood classifier using the original spectral bands) my not be capable of handling a training sample containing many land surface categories. Baatz and Schape (2000) noted that important semantic information for understanding an image is necessary through analyzing their mutual relations rather than single pixels.

All types of image features are textured in two ways. One is texture within a land-cover class (e.g., textures of grass, trees, roads, soil, water, and rooftops), and the other is the detailed land-cover objects and features from which a land-use can be inferred (e.g., the texture of a residential class) (Myint, 2006a; Myint et al., 2006). They both represent micro and macro textures that need to be considered at multiple scales. It is widely known that procedures for image segmentation using texture features are one of the main research topics in the area of image processing (Dong, 2000; Ferro and Warner, 2002; Chen et al., 2004).

It has been observed that several geospatial techniques have emerged as an alternative to spectral-based traditional classifiers: the image spatial co-occurrence matrix (Franklin et al., 2000);

local variance (Woodcock and Harward, 1992; Ferro and Warner, 2002; Stow et al., 2003); the variogram (De Jong and Burrough, 1995; Brown, 1998; Walsh et al., 2003); fractal analysis (Lam and Quattrochi, 1992; Bian and Walsh, 1993; Crews-Meyer, 2002; Read, 2003); and spatial auto-correlation (Emerson et al., 1999; Purkis et al., 2006). These approaches have demonstrated some improvements in the classification accuracy of urban land-covers and subsequent inference of urban land-use from land-cover classes. However, most of the geospatial approaches take spatial association of features at single scale and do not transform images into different spatial features and/or analyze texture features at multiple scales.

During the last decade, a powerful mathematical transformation technique called wavelet transforms has received a lot of attention by researchers in image processing because it analyzes signals at multiple scales. A number of researchers have demonstrated the power of wavelet transforms in image texture analysis and processing (Chang and Kuo, 1993; Zhu and Yang, 1998; Sheikholeslami et al., 1999; Bian, 2003). Myint et al. (2002) explored the effectiveness of a wavelet transform approach in discriminating urban land-use and land-cover samples. However, these studies used small subsets of pure land-use and land-cover classes without an operational algorithm for classification of the remotely sensed images. In other words, these studies did not deal with real-world situations, and samples used in the studies were all homogeneous classes of small subsets. In the previous study, there was no single sample that covered two or more land-use or land-cover classes in the way a local window moves throughout the image to identify the classes. In the real-world situation, operational texture-based algorithms employ a local window to classify real satellite images instead of treating some training samples as local windows to examine the effectiveness of potential classification algorithms in the preliminary stages of testing (Myint et al., 2006).

Myint (2006b) developed a number of operational algorithms and a wavelet-based classification framework to recognize spatial objects in satellite images. The objective of this study

is to examine and demonstrate the importance of level of scales (texture features at different spatial resolutions) in connection to consideration of a characteristic scale that can be defined as a minimum distance between two pixels to characterize a texture feature (Lark, 1996) using the algorithms developed by Myint (2006b). This study also demonstrates the impact of a local window on the classification accuracy when dealing with real-world situations in remotely sensed images instead of dealing with training samples or image subsets. Hence, different texture measures, different window sizes, and combinations of different decomposition levels using operational wavelet-based algorithms were tested in the study.

2. Study Area and Training Samples

A pan sharpened IKONOS image was acquired for Dallas, Texas on October 3, 2004. The image data are at 1-m spatial resolution with four channels: blue - B1 (0.45 – 0.52 μm), green - B2 (0.52 – 0.60 μm), red - B3 (0.63 – 0.69 μm), and near infrared (NIR) - B4 (0.76 – 0.90 μm). A subset of IKONOS data (1191x1478 pixels) covering a portion of the central part of the Dallas metropolitan area (Figure 1) was then used to examine and demonstrate the effectiveness of wavelets using different texture measures, local window sizes, and combinations of different decomposition levels.

An area covering five classes was subsequently selected to develop training samples, including commercial, grassland, forest, residential, and water. One training sample per class was selected for all classes. The selected training samples and their descriptive statistics are presented in Table 1. The standard deviation and coefficient of variation for the homogeneous classes (e.g., forest) were relatively low while the heterogeneous classes (e.g., residential) were much higher.

3. Methods

3.1. The Wavelet Approach

Mallat (1989) developed the multiresolution analysis theory using the orthonormal wavelet basis. The approximation and details of a two-dimensional image $f(x,y)$ at resolution 2^j can be defined by the coefficients computed by the following convolutions:

$$A^d_{2^j} f = ((f(x,y) * \phi_{2^j}(-x)\phi_{2^j}(-y))(2^{-j}n, 2^{-j}m))_{(n,m)\in Z^2} \quad (1)$$

$$D^1_{2^j} f = ((f(x,y) * \phi_{2^j}(-x)\psi_{2^j}(-y))(2^{-j}n, 2^{-j}m))_{(n,m)\in Z^2} \quad (2)$$

$$D^2_{2^j} f = ((f(x,y) * \psi_{2^j}(-x)\phi_{2^j}(-y))(2^{-j}n, 2^{-j}m))_{(n,m)\in Z^2} \quad (3)$$

$$D^3_{2^j} f = ((f(x,y) * \psi_{2^j}(-x)\psi_{2^j}(-y))(2^{-j}n, 2^{-j}m))_{(n,m)\in Z^2} \quad (4)$$

where integer j is a decomposition level, m, n are integers, $\phi(x)$ is a smoothing function which provides low frequency information (low-pass filter), and $\psi(x)$ is a differencing function which provides high frequency information (high-pass filter).

$\phi(x)$ and $\psi(x)$ can be defined as:

Dilation equation $\phi(t) = \sqrt{2}\sum_k c(k)\phi(2t-k)$ (5)

Wavelet equation $\psi(t) = \sqrt{2}\sum_k d(k)\phi(2t-k)$ (6)

For example, Haar wavelet transform has coefficients: $c(0) = c(1) = 1/\sqrt{2}$, $d(0) = 1/\sqrt{2}$, and $d(1) = -1/\sqrt{2}$. Thus, its dilation equation and wavelet equation can be expressed as:

$$\phi(t) = \phi(2t) + \phi(2t-1) \quad (7)$$

$$\psi(t) = \phi(2t) - \phi(2t-1) \quad (8)$$

(Strang and Nguyen 1997).

Using multi-resolution wavelet decomposition, four different types of texture information (four different sub-images) can be extracted from an image or from a local moving window of an image using low-pass (L) and high-pass (H) filters (Mallet, 1989). These are approximation (LL), horizontal detail (LH), vertical detail (HL), and diagonal detail (HH) sub-images. The approximation sub-image is a low-pass filtered image. The other sub-images known as detail sub-images contain high frequency information. The approximation sub-image (LL) is expressed as $A_{2^j}^d f$, horizontal detail sub-image (LH) as $D_{2^j}^1 f$, vertical detail sub-image (HL) as $D_{2^j}^2 f$, and diagonal detail sub-image as $D_{2^j}^3 f$ in the above formulae 1, 2, 3, and 4 respectively. An example illustrating wavelet decomposition at level 1 using a hypothetical image is shown in Figure 2. In the next level, the approximation sub-image is decomposed. We used Haar wavelet to extract four different types of texture information.

A low-pass filtered coefficient in a sub-image is obtained by dividing the sum of two adjacent pixel values by $\sqrt{2}$ whereas the high-pass filtered coefficient is obtained by dividing the difference between two adjacent pixel values by $\sqrt{2}$. This procedure can be applied to any of the sub-images for the next level of decomposition. In this study, decomposition was done iteratively to the approximation sub-images at each level. This is referred to as pyramidal multi-resolution decomposition (Strang and Nguyen 1997). The filtered versions of the sub-images are down-sampled by a factor of two, and the approach is known as dyadic transform. The down-sampled sub-images are a quarter of the original approximation image, and there is neither loss nor redundancy of information between the levels since it is an orthogonal wavelet. A simple procedure for computing one approximation and three detail sub-images of a 4x4 image using Haar wavelet transform is illustrated in Figure 3.

In applying the wavelet approach, there are four considerations: the wavelet function, the textural measures used to describe the decomposed images, the level of decomposition, and the

local window size. All four factors could affect the performance of the wavelet approach in identifying land-use and land-cover classes. In this paper, the wavelet function selected was Haar and the textural measures were log energy, Shannon's index, and energy, which allowed us to focus on the effects of scale (local window size and decomposition level) on the classification accuracy.

Texture Measures

Three spatial measures below: log energy (*LOG*), Shannon's index (*SHAN*), and energy (*ENG*, also known as *angular second moment*), were used to identify the spatial arrangements of the selected land-use and land-cover classes at different scales.

$$(1)\ LOG = \sum_{i=1}^{M}\sum_{j=1}^{N} \log(c(i,j)^2), \tag{9}$$

$$(2)\ SHAN = -\sum_{i=1}^{M}\sum_{j=1}^{N} c(i,j) * \log c(i,j)), \text{ and} \tag{10}$$

$$(3)\ ENG = \frac{1}{MN}\sum_{i=1}^{M}\sum_{j=1}^{N} |c(i,j)|, \tag{11}$$

where $c(i,j)$ is a wavelet coefficient of a sub-image with *M* rows and *N* columns at location *i* and *j* at one level.

Wavelet decomposition and computation of feature vectors were done for all selected training samples before starting the decomposition of the local window at the top left corner of the image and computing texture measure values of sub-images of that local window. If a sample image or a local window of an image is decomposed up to level *m*, the feature vector used in this study can be described as

$$[f_{LL-1}, f_{LH-1}, f_{HL-1}, f_{HH-1}, \ldots\ldots\ldots\ldots, f_{LH-m}, f_{LH-m}, f_{HL-m}, f_{HH-m}]^T$$

The distance between the feature vector of a local window and a set of certain texture samples of their feature vectors will lead to the supervised classification using Euclidean distance classifier.

Level of Scale

More levels of decomposition can be expected to increase the overall accuracy because more decompositions can extract a larger number of sub-images that obtain texture information in different directions at different scales but in the real-world application this may not be the case because texture features in a small sub-image may not provide any useful information that would increase the accuracy. In some cases this situation will create signature confusion that could lead to deterioration in accuracy. For example, if we decompose a 32x32 image to four levels, the last sub-image at the fourth level will contain 2x2 pixels. There may be no significant texture information in a 2x2 image, and inclusion of this sub-image in the classification may lead to lower overall accuracy.

A 95x95 window was used to test the accuracy of the combination of different scale levels (i.e., level 1, level 1–2, level 1–3, level 1–4, level 1–5, level 1–6) since it allows more decomposition levels than in 31x31 and 63x63 images but could be expected to have fewer problems with mixed boundaries than larger windows (i.e., 127x127, 159x159).

Local Window Size

Windows are commonly used in digital image processing to determine the local information content around a pixel. It could be expected that the accuracy should increase with a larger local window size since it contains more information than a smaller window size and therefore provides more complete coverage of spatial variation, directionality, and spatial periodicity of a particular texture. If our objective is to identify residential classes a local window should be large enough to cover single-family houses, lawns, shrubs, trees, tar roads, and cement roads, concrete sidewalks, swimming pools, etc.

Gong and Howarth (1990) generated edge-density images with the use of sizes varying from 7x7 to 31x31. The most common approach for determining the appropriate window size is based on empirical results using automated classifications (Hodgson, 1998). The seminal works on second-order texture statistics by Haralick et al. (1973) were based on windows of 64x64 or 20x50. Pesaresi (2000) experimented with 47 different square window sizes, ranging from 5x5 to 99x99. It is important to note that the identification of a method for determining optimal window size a priori classification is ambiguous (Gong and Howarth, 1992).

In this study, the evaluation of different window sizes was performed in order to determine the optimal window size and examine the impact of classification specificity on the selection of local window size in real-world applications. It should be noted that larger local window sizes might provide higher accuracies since they cover more features and objects. In general, information contained in a 159x159 local window (159x159=25,281 pixels) is about 26 times greater than a 31x31 window (31x31=961 pixels). However, the above statement may only be true if a particular technique can be used effectively to characterize spatial arrangements of features at multiple scales. Some spatial analysis methods may not improve accuracy while using a larger window size since they focus primarily on coupling between features and objects at single scale and cannot determine the effective representative index of particular texture features (Myint et al., 2004).

There have been some attempts to improve the traditional spectral-based classifiers by using texture transforms in which some measure of variability in digital number (DN) values is estimated within local windows, for example, in the contrast between neighboring pixels (Edwards et al., 1988). One commonly used statistical procedure for analyzing texture uses the image standard deviation or variance (Woodcock and Harward, 1992; Arai, 1993; De Jong and Burrough 1995; Ferro and Warner, 2002; Stow et al., 2003). It should be noted that different texture features may share the same standard deviation or variance, and the same spatial index (e.g., fractal dimension value) (Dong, 2002). These texture algorithms may also share the same or similar index

values for different window sizes of the same texture class. For example, different window sizes of a deterministic texture will give the same standard deviation value. A larger window size may not improve classification accuracy while using a simple statistical measure to characterize texture features. In this study, we used some texture samples of land-use land-cover classes to demonstrate the effectiveness of a commonly used statistic (i.e., variance) to characterize spatial arrangements of features and objects when dealing with different window sizes of homogeneous texture features (a subset or a region does not contain more than one texture feature). We also attempted to determine if larger windows improve classification accuracy while using the wavelet technique.

To demonstrate the impact of local window sizes on the classification accuracy when using homogeneous texture features, linear discriminant analysis approach was employed. The texture measures (i.e., energy values of the decomposed sub-images) from the wavelet analysis and the variance values of the samples generated above were subject to discriminant analysis. SPSS software package was used to perform discriminant analysis for the classification of land-use and land-cover samples. The procedure generates a discriminant function (or, for more than two groups, a set of discriminant functions) based on linear combinations of the predictor variables, which provide the best discrimination between the groups.

To understand the nature of the choice of a local window to identify selected land-use and land-cover classes, image samples covering 16x16, 32x32, 64x64, 128x128, and 256x256 pixels or local window sizes are provided in Figure 4. It can be observed that the larger the local windows, the higher the chance of covering more land-use and land-cover classes, and objects.

The smallest window size used in this study was 31x31 since it was anticipated that data obtained from a local window size of less than 31x31 (31 m) for an IKONOS 1 m resolution may not be large enough to cover and identify a residential class since the window size needs to cover land surface features within a residential area (e.g., rooftops, lawns, shrubs, trees, tar roads, cement roads, sidewalks, driveways, and swimming pools). The local window sizes (w) used in this study

include 31x31, 63x63, 95x95, 127x127, and 159x159. To examine the relation between local window sizes and classification accuracy when dealing with homogeneous texture features we generated five samples each of the selected land-use and land-cover classes for the above local window sizes (31x31, 63x63, 95x95, 127x127, and 159x159) using IKONOS band 3 data.

The difference between each window and its consecutive window is 32 pixels since it is understood that there is no significantly different information contained in an area of less than 32x32 m on the ground. We added 32 to make the number of pixels in successive windows odd since the identified class needs to be assigned to the center of the window. However, the algorithm automatically adds one row and one column for odd number windows or sub-images of the selected windows using mirror extension during computation since wavelet decomposition procedure is done with even number signals (i.e., rows or columns). Hence, during the wavelet computation the actual local windows used will be 32x32, 64x64, 96x96, 128x128, and 160x160.

The extension is done only during the computation process and the identified class is assigned to the center of the original local window. Since (w-1)/2 pixels are lost at the top, bottom, left, and right of the entire image, the algorithm automatically extends (w-1)/2 pixels all around the image (e.g., 16 pixels for a 33x33 local window) before starting the whole process. The extension is done using the mirror extension.

Classifier

The Euclidean distance classifier was employed for texture classification using the computed texture feature vector of a local window and training samples. Each pattern class C_k is represented by a prototype pattern P_k. If decomposition was done up to three levels for four bands, we would obtain 48 different sub-images for one training sample or one local window and hence, P_k (k = 1, 2… 48) were total feature vectors of the training samples. The Euclidean distance classifier assigns an unknown class pattern Q (local window) to the class (one of the training samples) if the distance

R_j between Q and P_k is the minimum among all possible class prototypes. The Euclidean distance is defined as

$$R_j = \|Q - P_k\| = \sqrt{\sum (q_k - p_{k,j})^2} \,. \quad (12)$$

where j was a class sample (i.e., j = 1, 2 , 3, 4, 5).

3.2. Accuracy Assessment

It is generally accepted that a minimum of 50 sample points for each land-use land-cover category in the error matrix should be collected (Congalton, 1991; Congalton and Green, 1999). For example, if we had selected 50 sample points per class, the total points selected would have been only 0.014% of the whole image (i.e., 250 out of 1191 x 1478 = 1,760,298 points). Uncertainty of the overall picture does not allow us to assume that the sample points (0.014% of the entire scene) perfectly represent the whole image for accuracy assessment. For an ideal evaluation and a precise comparison, especially when dealing with the evaluation of different classification approaches, it is generally accepted that such "wall-to-wall" comparisons of checking every pixel in an image is the best approach (Lillesand et al., 2004).

Hence, the classes were accurately delineated using manual interpretation with heads-up digitizing using the ERDAS Imagine raster tool option. All points or pixels (i.e., 1191 x 1478 = 1,760,298 pixels) in the visually interpreted map were used to assess the accuracy instead of selecting a certain number of pixels using random, stratified random, or systematic sampling approaches. This is to accurately determine which one of the decision rules, window sizes, combination of levels, and texture measures in comparison to geospatial and traditional approaches employed in the study can effectively identify the urban land-use and land-cover classes that we can easily recognize with our eyes.

The output map for accuracy assessment generated from manual interpretation is assumed to be error-free or at least highly accurate with negligible error because of the thorough digitization procedure done with the help of sound local area knowledge and a comprehensive ground survey. The manually digitized map (Figure 5) was treated as the reference data (ground truth data).

A diagram illustrating the research design employed in this study is presented in Figure 6. Image display, training sample selection, statistical analysis, layer stack, band split, image subset, and data import/export were accomplished using ERDAS Imagine software. However, all wavelet-based approaches for texture analysis and image classification were developed using C++ programming language.

4. Results and Discussion

Local Window with Homogeneous Texture Training Samples

It can be observed from Table 2 that larger window sizes do not improve classification accuracy while using variance measure to characterize homogeneous texture features. In general, all window sizes produced very low accuracies and overall accuracies for all window sizes are inconsistent with varying window sizes. The overall classification accuracy for 31x31, 63x63, 95x95, 127x127, and 159x159 homogeneous land-use and land-cover samples were found to be 24%, 20%, 48%, 24%, and 40% respectively (Table 2). The 95x95 local window size achieved the highest overall accuracy (48%) and the highest Kappa coefficient (0.35). It is difficult to interpret the producer's and user's accuracies since they range from 0% to 100%, and all local window sizes produced at least two 0% producer's or user's accuracy for all windows. For example, producers' and users' accuracies for forest, grass, and residential classes were found to be 0% for a 31x31 local window. The resulting overall accuracies have no relationship with the local window sizes used. Like many other texture and spatial analysis approaches, variance of land-use and land-cover classes in texture analysis

focuses only on coupling between features and objects at single scale and is not capable of splitting signals into different transformed features in different directions at multiple scales. The variance measure cannot characterize particular texture features according to their directionality, spatial arrangements, variations, edges, repetitive nature of objects and features within a texture set, and contrasts.

As anticipated, the wavelet approach with the use of energy measure consistently improved the overall accuracy of 76%, 88%, 88%, 96%, and 100% for 31x31, 63x63, 95x95, 127x127, and 159x159 local window sizes respectively (Table 3). The kappa coefficients for 31x31, 63x63, 95x95, 127x127, and 159x159 window sizes were found to be 0.70, 0.85, 0.85, 0.95, and 1.00 respectively. This is the result for the different window sizes of the samples using energy measure of wavelet sub-images at 2 levels and a discriminant function. This clearly demonstrates that the overall accuracy and Kappa coefficient increase as the local window sizes increase for homogeneous textures of land-use and land-cover classes for wavelet transforms (Table 3). This is because the wavelet technique extracts four different spatial features at each scale level from images and the selected samples are homogeneous texture features of land-use and land-cover classes that contain only one class per sample. A larger window size for all classes resulted in constantly increasing producer's and user's accuracies. There may be some signature confusion between forest and grassland since producer's and user's accuracies of these classes were relatively low for smaller window sizes. However, this is not the case for larger window sizes, and the 159x159 produced 100% producer's and user's accuracies for all classes. Hence, this study confirms that larger windows improve the classification accuracy.

Texture Measures

63x63 training samples (or local windows) were used to test the accuracy of different texture measures (Table 4). This classification was carried out with the use of the entire image under study

using the wavelet algorithm developed in this study for the real-world situation. From Table 4 it can be observed that energy is probably the most effective measure since it gave the highest overall accuracy (81.84%). The same measure got the highest Kappa coefficient (0.68), which implies that an observed classification is on average 68% more accurate than one resulting from chance. Shannon's index was the least accurate measure since it gave the lowest overall accuracy (30.17%). The Kappa coefficient for Shannon's index is 0.17.

The lowest producer's accuracy (4.35%) and user's accuracy (14.587%) were given by residential class and grassland respectively, and Shannon's index yielded the lowest producer's and user's accuracies. This may be due to some signature confusion between the classes since there is a lot of grass in residential areas, and their spatial arrangements in some cases might be similar. The other classes that produced very low producer's accuracies were commercial (22.99% for log energy) and grassland (36.55% for log energy), and very low user's accuracies for forest (47.51% for Shannon's index) and residential (25.95% for Shannon's index). This could be due to the fact that Shannon index my not be effective in characterizing complex spatial features.

Local Window with Real-world Images

The best texture measure (i.e., energy) obtained from the 63x63 samples was used to test the accuracy of different window sizes (i.e., 31x31, 63x63, 95x95, 127x127, 159x159). It can be observed from Table 5 that the 63x63 window was the optimal window for this study since it produced the highest overall accuracy (81.84%) and the highest Kappa coefficient (0.68). This is because the minimum distance between two pixels to cover a texture (the characteristic scale) is approximately 60 m on the ground for the residential class. The residential class contains the most complex texture since residential areas are composed of a diversity of spectrally different materials concentrated in a small area (e.g., plastic, metal, rubber, glass, cement, wood, shingle, sand, gravel,

brick, stone, soil, vegetation, water, etc.). For example, tar roads, cement roads, rooftops with different materials (e.g., tile roof, wood, shingle roof, metal roof, tar roof, glass roof, plastic roof, light-gray asphalt roof), grasses, trees, bare soil, shrubs, swimming pools, driveways, sidewalks, may have a completely different spectral response, but together they are considered as a residential class. Apparently, this is not the case for all other classes. This indicates that the characteristic scale of the most complex class is the optimal window to achieve the highest classification accuracy. The output map of energy measure using a 63x63 window (Figure 7) looks informative and similar to the reference map (Figure 6). This study suggests that a larger window does not necessarily produce higher accuracy when dealing with a real-world situation.

In general, the accuracy should increase with a larger local window size since it contains more information. This condition is true when dealing with homogeneous texture features (deterministic texture). However, in the real-world situation we are dealing with two or more different land-use and land-cover classes (two or more different texture features) in most cases while the local window moves throughout the image for classification. From a computational perspective, the ideal window size is the smallest size that also produces the highest accuracy (Hodgson, 1998). It is important to note that minimization of local window size is also important in image texture and pattern recognition techniques since larger window size tends to cover more land-use and land-cover features and it consequently creates mixed boundary pixels or mixed land-use and land-cover problems. This may be partly because characteristic scales of different land-use and land-cover classes could be greatly different (e.g., characteristic scales of residential and water).

It can be observed from Table 5 that the overall accuracy consistently decreases with increasing window sizes (77.39% for 95x95, 76.66% for 127x127, 74.32% for 159x159), but only after it reaches its maximum accuracy at the optimum window (63x63). Another problem of using larger window size is the fact that smaller land-use and land-cover features will be lost in classification. In other words, the larger the window size the smaller the number of segmented

regions or land-use and land-cover features identified in the image. It will also maximize the number of missing pixels around the edges of the image. In this study, the largest window (i.e., 159x159) gave the lowest overall accuracy (74.32%) and the lowest Kappa coefficient (0.50).

The second lowest accuracy was produced by a 33x33 local window. This was because a 33x33 local window may not be large enough to completely cover heterogeneous classes (e.g., residential, commercial). It was found that the commercial class produced the lowest producer's accuracies (31.16% for a 127x127 window and 20.67% for a 159x159 window) and grassland yielded the lowest user's accuracy (34.14%). In fact, the second lowest accuracy was the producer's accuracy given by the commercial class when using a 127x127 window (31.16%). In general, commercial and grassland classes were again found to be weak in using different window sizes since they gave relatively low producer's and user's accuracies. The local window needs to be large enough to cover spatial features that represent selected land-use classes. However, it is important to note that there is no optimal window size that is suitable for all applications.

Combination of Scale Levels

We employed the 95x95 window using the best texture measure (i.e., energy) to test the accuracy of different combinations of decomposition levels. It was found that a combination of level 1–4 produced the highest overall accuracy for the 95x95 window in this study. From Table 6, it can be observed that the accuracy increases with the increase in the number of levels until it reaches four levels (76.60% for 1 level, 77.39% for 2 levels, 78.20% for 3 levels, 78.89% for 4 levels), and accuracy decreases with increasing number of levels after that (77.76% for 5 levels, 75.06% for 6 levels). It implies that sub-images at level five (6x6 pixels) and level six (3x3 pixels) do not contain useful information on textures of selected land-use and land-cover classes. The lowest Kappa coefficient (0.55) was given by a combination of level 1–6. This is because a smaller image has less texture information. For example, 2x2 pixel images of grassland, woodland, and water could be

similar or closely related. The lowest producer's accuracy was again given by the commercial class (43.11% for L1-6) and the lowest user's accuracy was given by grassland (36.94% for L1-6) (Table 6). It was observed from Table 6 that commercial and grassland areas generally gave low accuracies.

5. Conclusion

The energy measure gave the highest accuracy among all texture measures computed from the wavelet-decomposed images. Results from this study show that the choice of window size affects the classification accuracy. The selection of local window size depends on several factors such as image resolution, nature of the study area, number of classes, training sample selection, spectral resolution, spatial techniques, and decomposition level employed. The highest overall accuracy for the 95x95 window was achieved by a combination of level 1–4 in this study. This implies that smaller sub-images at the last two levels (two steps before reaching its maximum level) do not contain useful information on textures of selected land-use and land-cover classes. This finding is not consistent with the results from the previous study (Myint et. al., 2004) since this study employed the original image instead of using homogeneous texture samples. It may not be appropriate to consider a local window size smaller than the minimum distance between two pixels to characterize the most heterogeneous class (e.g., residential). The 63x63 window size (~ 60 m) for an IKONOS 1 m resolution data was found to be the optimal window for urban land-use and land-cover classification. This distance is the approximate characteristic scale (minimum distance between two pixels to cover a texture) for the residential class that is considered the most heterogeneous class among the selected land-use and land-cover classes.

Some of the crucial findings of the study can be summarized as follows.

The classification accuracy can be improved by using more combinations of sub-images at different scales. It should be noted that larger window sizes allow more combinations of scale levels and hence, produce more texture-transformed sub-images. Myint et. al. (2002) demonstrated that the combination of more levels improve the classification accuracy significantly when using homogeneous texture samples. However, a higher level of decomposition may not always improve the overall accuracy. This is because a very small sub-image does not contain enough information to represent texture features of selected classes, and this could consequently degrade the overall accuracy. It is important to note that decomposition should not exceed a level of scale at which the sub-image is less than eight pixels. This could be a general rule of thumb for most applications.

The variance measure not only gave very low classification accuracy but also showed no relation with the increasing window size. This study demonstrates that variance values of texture features are ineffective in characterizing land-use and land-cover classes. This could also be true for some other spatial measures such as spatial autocorrelation and fractals that focus only on coupling between features and objects at single level and are not capable of transforming signals at multiple scales.

Larger window sizes consistently and significantly improve the overall classification accuracy when dealing with homogeneous texture samples (one texture class per sample). This result does not concur with other studies that small window sizes yield higher classification accuracies in urban land cover classification (Gong and Howarth, 1992; Chen *et al*., 2004). This is because this study includes complex land-use classes (i.e., residential, commercial) the other studies consider land covers only.

In the real-world situation, a larger window may not necessarily produce higher accuracy, and hence, an optimal window needs to be determined. A larger window tends to cover more land-use and land-cover classes and therefore may miss smaller regions of classes that could lead to

poorer accuracy whereas a smaller window tends to be incomplete in its coverage of texture features that represent a class.

The characteristic scale (minimum distance between two pixels to cover a particular class) of the most complex class (texture feature) among all selected land-use and land-cover classes could be an important factor to be considered for a better classification accuracy.

Acknowledgement

This research has been supported by the National Science Foundation (grant # 0351899). The author wishes to thank Gautam Gudhar and Liran Ma for their assistances in coding the algorithms.

References:

BAATZ, M. and SCHAPE, A., 2000, Multiresolution Segmentation: an optimization approach for high quality multi-scale image segmentation. *Proceedings of Angewandte Geogr. Informationsverarbeitung XII*, Strobl, J. and Blaschke, T. eds., Wichmann, Heidelberg, pp. 12-23.

BARNSLEY, M. J., BARR, S. L. and SADLER, G. J., 1991, Spatial re-classification of remotely sensed images for urban land-use monitoring. *Proceedings of Spatial Data 2000*, Oxford, 17-20 September, Remote Sensing Society, Nottingham, pp. 106-117.

BERGEN, J. R., and JULESZ, B., 1983, Rapid discrimination of visual patterns. IEEE Transactions on Systems, Man, and Cybernetics, **13**, 857–863.

BIAN, L., 2003, Retrieving urban objects using a wavelet transform approach. *Photogrammetric Engineering and Remote Sensing*, **69**, 133-141.

BIAN, L. and WALSH, S. J., 1993, Scale dependencies of vegetation and topography in a mountainous environment of Montana. *Professional Geographer*, **45**, 1-11.

BROWN, D. G., 1998, Classification and boundary vagueness in mapping presettlement forest types. *International Journal of Remote Sensing*, **12**, 105-129.

CAMPBELL, J., 2002, *Introduction to Remote Sensing*, 3rd edition, The Guilford press, New York, p 620.

CHANG, T. and KUO, C.-C.J., 1993, Texture analysis and classification with tree-structured wavelet transform. *IEEE Transactions on Image Processing*, **2**, 429-441.

CHEN, D. and STOW, D. A., 2003, Strategies for Integrating Information from Multiple Spatial Resolutions into Land-Use/Land-Cover Classification Routines. *Photogrammetric Engineering and Remote Sensing*, **69**, 1279-1287.

CHEN, D., STOW, D. A. and GONG, P., 2004, Examining the effect of spatial resolution and texture window size on classification accuracy: an urban environment case. *International Journal of Remote Sensing*, **25**, 2177-2192.

CONGALTON, R. G., 1991, A review of assessing the accuracy of classifications of remotely sensed data," *Remote Sensing of Environment*, **37**, 35-46.

CONGALTON, R. G. and GREEN, K., 1999, *Assessing the Accuracy of Remotely Sensed Data*: *Principles and Practices* Lewis Publishers, Boca Raton, Florida, 137 p.

CREWS-MEYER, K. A., 2002, Characterizing landscape dynamism using paneled-pattern metrics. *Photogrammetric Engineering and Remote Sensing*, **68**, 1031-1040.

DE JONG, S. M. and BURROUGH, P. A., 1995, A Fractal Approach to the classification of Mediterranean Vegetation Types in Remotely Sensed Images. *Photogrammetric Engineering and Remote Sensing*, **61**, 1041-1053.

DONG, P., 2000, Lacunarity for Spatial Heterogeneity Measurement in GIS. *Geographic Information Sciences*, **6**, 20-26.

EMERSON, C. W., LAM, N. S. N. and QUATTROCHI, D. A., 1999. Multi-Scale fractal analysis of image texture and pattern. *Photogrammetric Engineering and Remote Sensing*, **65**, 51-61.

FERRO, C. J. S. and WARNER, T. A., 2002, Scale and texture in digital image classification. *Photogrammetric Engineering and Remote Sensing*, **68**, 51-63.

FOSTER, B. C., 1985, An examination of some problems and solutions in monitoring urban areas from satellite platforms. *International Journal of Remote Sensing*, **6**, 139-151.

GONG, P. and HOWARTH, P. J., 1990, The use of structural information for improving land cover classification accuracies at the rural urban fringe. *Photogrammetric Engineering and Remote Sensing*, **56**, 67-73.

FRANKLIN, S. E., HALL, R. J., MOSKAL, L. M., MAUDIE, A. J. and LAVIGNE, M. B., 2000, Incorporating texture into classification of forest species composition from airborne multispectral images. *International Journal of Remote Sensing*, **21**, 61-79.

GONG, P. and HOWARTH, P. J., 1990, The use of structural information for improving land cover classification accuracies at the rural urban fringe. *Photogrammetric Engineering and Remote Sensing*, **56**, 67-73.

---------- , 1992, Frequency based contextual classification and gray level vector reduction for land use identification. *Photogrammetric Engineering and Remote Sensing*, **58**, 423-437.

HARALICK, R. M., SHANMUGAN, K. and DINSTEIN, J., 1973, Textural features for image classification. *IEEE Transaction on Systems, Man, and Cybernetics*, **SMC-3**(6), 610-621.

HODGSON, M. E., 1998, What size window for image classification? A cognitive perspective. *Photogrammetric Engineering and Remote Sensing*, **64**(8), 797-807.

JENSEN, J. R. and COWEN, D. C., 1999. Remote sensing of urban/suburban infrastructure and socio-economic attributes. *Photogrammetric Engineering and Remote Sensing*, **65**, 611-622.

LAM, N. S. N. and QUATTROCHI, D.A., 1992. On the issues of scale, resolution, and fractal analysis in the mapping sciences. *Professional Geographer*, **44**, 88-97.

LARK, R. M., 1996, Geostatistical description of texture on an aerial photograph for discriminating classes of land cover. *International Journal of Remote Sensing*, **17**, 2115-2133.

LILLESAND, T. M., KIEFER, R. W. and CHIPMAN, J. W., 2004, *Remote Sensing and Image Interpretation*, 5th edition, John Wiley and Sons, New York, 763 p.

MALLAT, S. G., 1989, A Theory for multi-resolution signal decomposition: the wavelet representation. *IEEE Transactions on Pattern Analysis and Machine Intelligence*, **11**, 674-693.

METZGER, J. P. and MULLER, E., 1996, Characterizing the complexity of landscape boundaries by remote sensing. *Landscape Ecology*, **11**, 65-77.

MYINT, S.W., 2006a, Urban Mapping with Geospatial Algorithms, *Urban Remote Sensing* (Qihao Weng and Dale Quattrochi, editors), Taylor and Frances, pp. 109-135.

MYINT, S.W., 2006b, A New Framework for Effective Urban Land Use Land Cover Classification: A Wavelet Approach. *GIScience and Remote Sensing*, **43**, 155-178.

MYINT, S. W., LAM, N. S. N. and TYLER, J., 2002, An evaluation of four different wavelet decomposition procedures for spatial feature discrimination within and around urban areas. *Transactions in GIS*, **6**, 403-429.

MYINT, S. W., LAM, N. S. N. and TYLER, J., 2004, Wavelet for urban spatial feature discrimination: comparisons with fractal, spatial autocorrelation, and spatial co-occurrence approaches. *Photogrammetric Engineering and Remote Sensing*, **70**, 803-812.

MYINT, S.W., MESEV, V. and LAM, N.S.N, 2006, Texture Analysis and Classification Through A Modified Lacunarity Analysis Based on Differential Box Counting Method. *Geographical Analysis*, **38**, 371-390.

PESARESI, M., 2000, Texture analysis for urban pattern recognition using fine-resolution panchromatic satellite imagery. *Geographical and Environmental Modelling*, **4**, 43-63.

PURKIS, S. J., MYINT, S. W. and RIEGL, B. M., 2006, Enhanced detection of the coral *Acropora cervicornis* from satellite imagery using a textural operator. *Remote Sensing of Environment*, **101**, 82-94.

READ, J., 2003, Spatial analyses of logging impacts in Amazonia using remotely sensed data. *Photogrammetric Engineering and Remote Sensing*, **69**, 275-282.

SADLER, G. J., BARNSLEY, M. J. and BARR, S. L., 1991, Information extraction from remotely-sensed images for urban land analysis. *Proceedings of the Second European Conference on Geographical Information Systems (EGIS'91)*, Brussels, Belgium, April, EGIS Foundation, Utrecht, pp. 955-964.

SHEIKHOLESLAMI, G., ZHANG, A. and BIAN, L., 1999, A multi-resolution content-based retrieval approach for geographic images. *Geoinformatica,* **3**(2):109-139.

STOW, D., COULTER, L., KAISER, J., HOPE, A., SERVICE, D., SCHUTTE, K. and A. WALTERS, 2003, Irrigated vegetation assessment for urban environments. *International Journal of Remote Sensing*, **69**, 381-390.

STRANG, G. and NGUYEN, T., 1997, *Wavelets and Filter Banks*. Wellesley-Cambridge Press, revised edition, 1997, Wellesley, MA, USA, 520 p.

WALSH, S. J., BIAN, L., MCKNIGHT, S., BROWN, D. G. and HAMMER, E. S., 2003, Solifluction steps and risers, Lee Ridge, glacier national park, Montana, USA: a scale and pattern analysis. *Geomorpholog*, **1399**, 1-18.

WOODCOCK, C. and HARWARD, V. J., 1992, Nested-hierarchical scene models and image segmentation. *International Journal of Remote Sensing*, **13**, 3167-3187.

ZHU, C. and YANG, X., 1998, Study of remote sensing image texture analysis and classification using wavelet. *International Journal of Remote Sensing*, **13**, 3167-3187.

MYINT, S.W., 2006a, Urban Mapping with Geospatial Algorithms, *Urban Remote Sensing* (Qihao Weng and Dale Quattrochi, editors), Taylor and Frances, pp. 109-135.

MYINT, S.W., 2006b, A New Framework for Effective Urban Land Use Land Cover Classification: A Wavelet Approach. *GIScience and Remote Sensing*, **43**, 155-178.

MYINT, S. W., LAM, N. S. N. and TYLER, J., 2002, An evaluation of four different wavelet decomposition procedures for spatial feature discrimination within and around urban areas. *Transactions in GIS*, **6**, 403-429.

MYINT, S. W., LAM, N. S. N. and TYLER, J., 2004, Wavelet for urban spatial feature discrimination: comparisons with fractal, spatial autocorrelation, and spatial co-occurrence approaches. *Photogrammetric Engineering and Remote Sensing*, **70**, 803-812.

MYINT, S.W., MESEV, V. and LAM, N.S.N, 2006, Texture Analysis and Classification Through A Modified Lacunarity Analysis Based on Differential Box Counting Method. *Geographical Analysis*, **38**, 371-390.

PESARESI, M., 2000, Texture analysis for urban pattern recognition using fine-resolution panchromatic satellite imagery. *Geographical and Environmental Modelling*, **4**, 43-63.

PURKIS, S. J., MYINT, S. W. and RIEGL, B. M., 2006, Enhanced detection of the coral *Acropora cervicornis* from satellite imagery using a textural operator. *Remote Sensing of Environment*, **101**, 82-94.

READ, J., 2003, Spatial analyses of logging impacts in Amazonia using remotely sensed data. *Photogrammetric Engineering and Remote Sensing*, **69**, 275-282.

SADLER, G. J., BARNSLEY, M. J. and BARR, S. L., 1991, Information extraction from remotely-sensed images for urban land analysis. *Proceedings of the Second European Conference on Geographical Information Systems (EGIS'91)*, Brussels, Belgium, April, EGIS Foundation, Utrecht, pp. 955-964.

SHEIKHOLESLAMI, G., ZHANG, A. and BIAN, L., 1999, A multi-resolution content-based retrieval approach for geographic images. *Geoinformatica,* **3**(2):109-139.

STOW, D., COULTER, L., KAISER, J., HOPE, A., SERVICE, D., SCHUTTE, K. and A. WALTERS, 2003, Irrigated vegetation assessment for urban environments. *International Journal of Remote Sensing*, **69**, 381-390.

STRANG, G. and NGUYEN, T., 1997, *Wavelets and Filter Banks*. Wellesley-Cambridge Press, revised edition, 1997, Wellesley, MA, USA, 520 p.

WALSH, S. J., BIAN, L., MCKNIGHT, S., BROWN, D. G. and HAMMER, E. S., 2003, Solifluction steps and risers, Lee Ridge, glacier national park, Montana, USA: a scale and pattern analysis. *Geomorpholog*, **1399**, 1-18.

WOODCOCK, C. and HARWARD, V. J., 1992, Nested-hierarchical scene models and image segmentation. *International Journal of Remote Sensing*, **13**, 3167-3187.

ZHU, C. and YANG, X., 1998, Study of remote sensing image texture analysis and classification using wavelet. *International Journal of Remote Sensing*, **13**, 3167-3187.

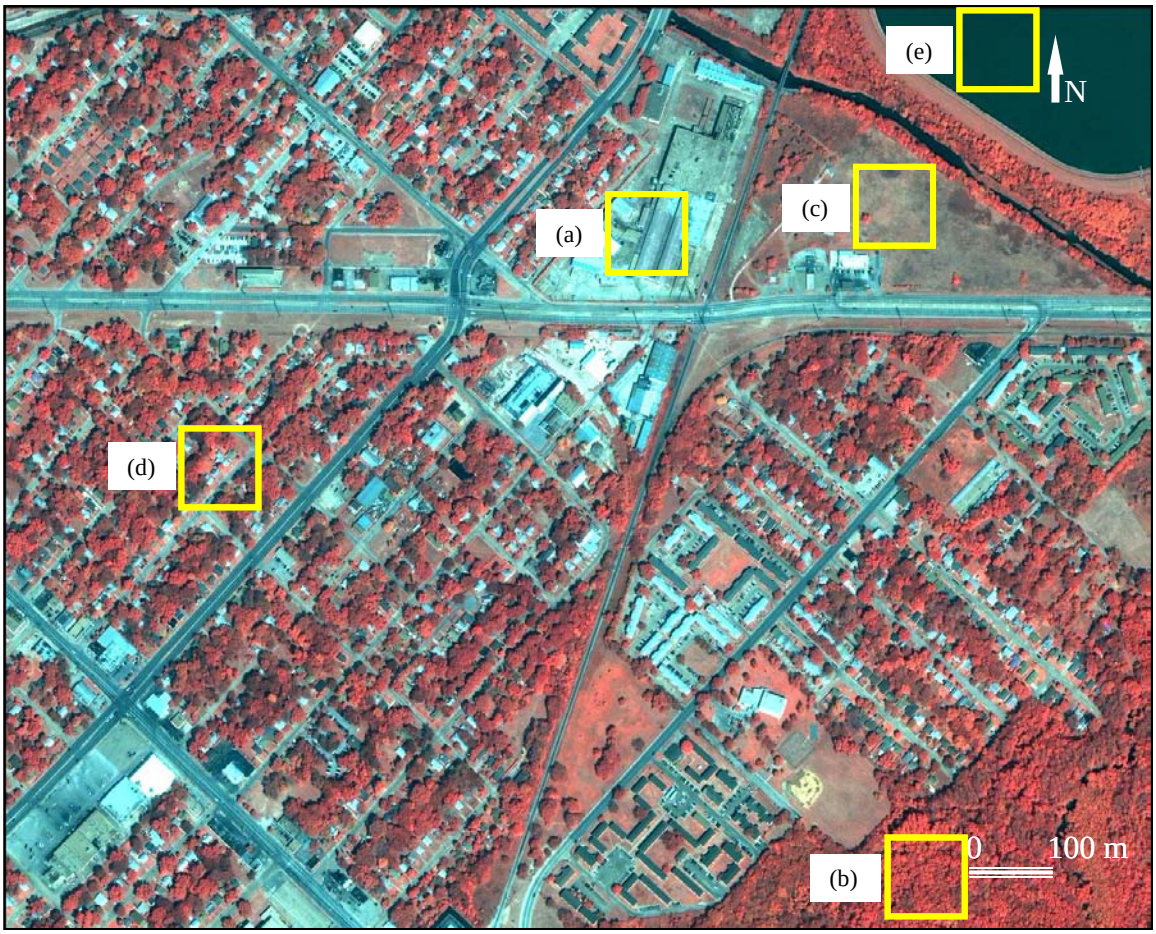

Figure 1. A false color composite of IKONOS 1 meter resolution data displaying channel 4 (0.76 – 0.90 μm) in red, channel 3 (0.63 – 0.69 μm) in green, and channel 2 (0.52 – 0.60 μm) in blue. Positions of the selected training samples (i.e., 95x95): (a) commercial; (b) forest; (c) grassland; (d) residential; (e) water.

Table 1. Descriptive statistics of the training samples displayed in Figure 2. Note: CV = coefficient variation; C = commercial; F = forest; G = grassland; R = residential; W = water.

	C	F	G	R	W
Band1					
Mean	521.09	338.96	417.95	396.09	321.34
Standard Deviation	112.26	44.00	20.91	74.62	6.29
CV	21.54	12.98	5.00	18.84	1.96
Band2					
Mean	618.23	350.32	492.21	433.79	323.87
Standard Deviation	157.69	65.52	35.47	114.88	8.72
CV	25.51	18.70	7.21	26.48	2.69
Band3					
Mean	523.59	228.86	448.32	325.05	145.37
Standard Deviation	158.20	73.33	38.02	129.41	9.80
CV	30.21	32.04	8.48	39.81	6.74
Band4					
Mean	527.57	733.41	611.74	597.32	75.97
Standard Deviation	145.59	136.66	61.44	184.45	10.75
CV	27.60	18.63	10.04	30.88	14.15

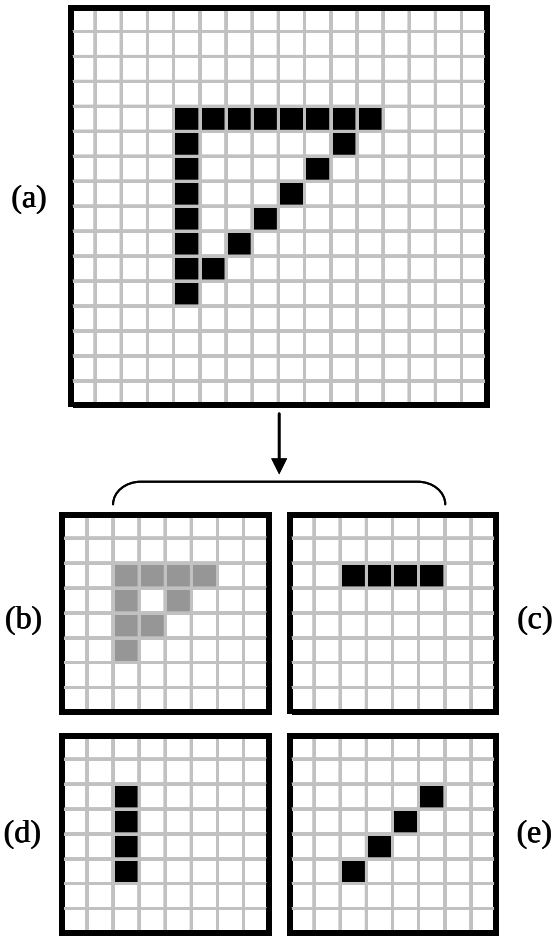

Figure 2. An example illustrating wavelet decomposition at level 1 using a hypothetical image: (a) original image; (b) approximation sub-image (LL); (c) horizontal detail sub-image (LH); (d) vertical detail sub-image (HL); (e) diagonal detail sub-image (HH). Note. down sampled sub-images (b, c, d, e) are a quarter of the preceding image (a).

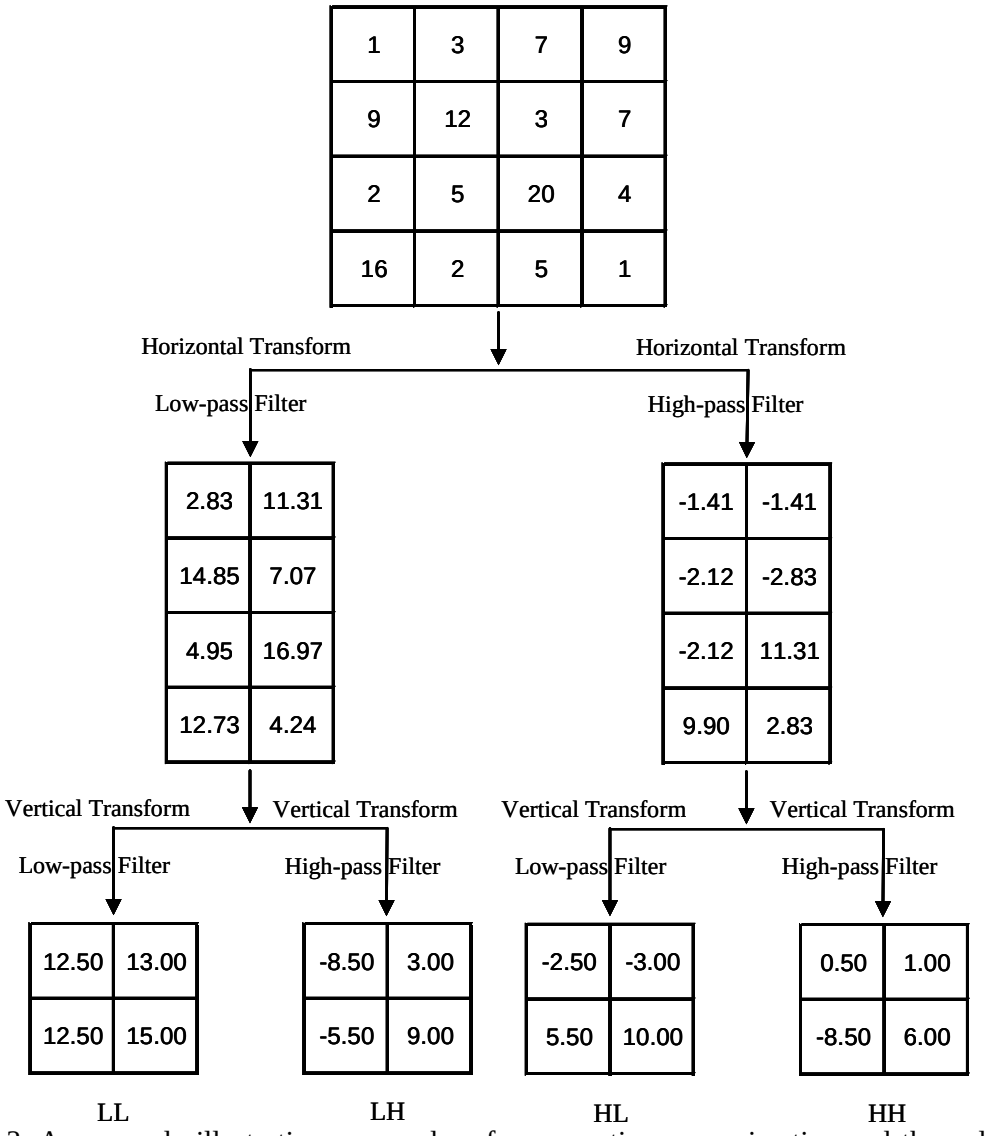

Figure 3. An example illustrating a procedure for computing approximation and three detail sub-images of a 4 by 4 image at level 1 using Haar wavelet transform: LL = approximation sub-image; LH = horizontal detail sub-image; HL = vertical detail sub-image; HH diagonal detail sub-image.

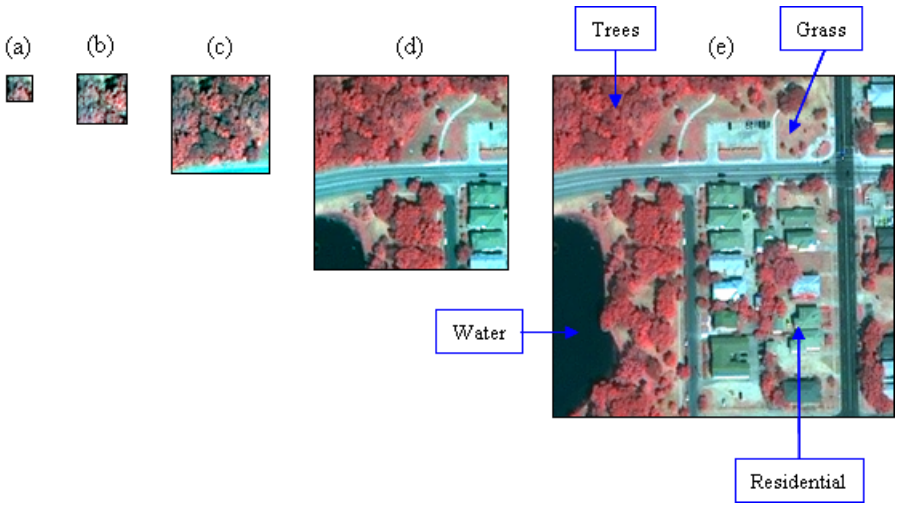

Figure 4. Image samples covering (a) 16x16, (b) 32x32, (c) 64x64, (d) 128x128, and (e) 256x256 pixels or local window sizes.

Figure 5. Manually interpreted and digitized map.

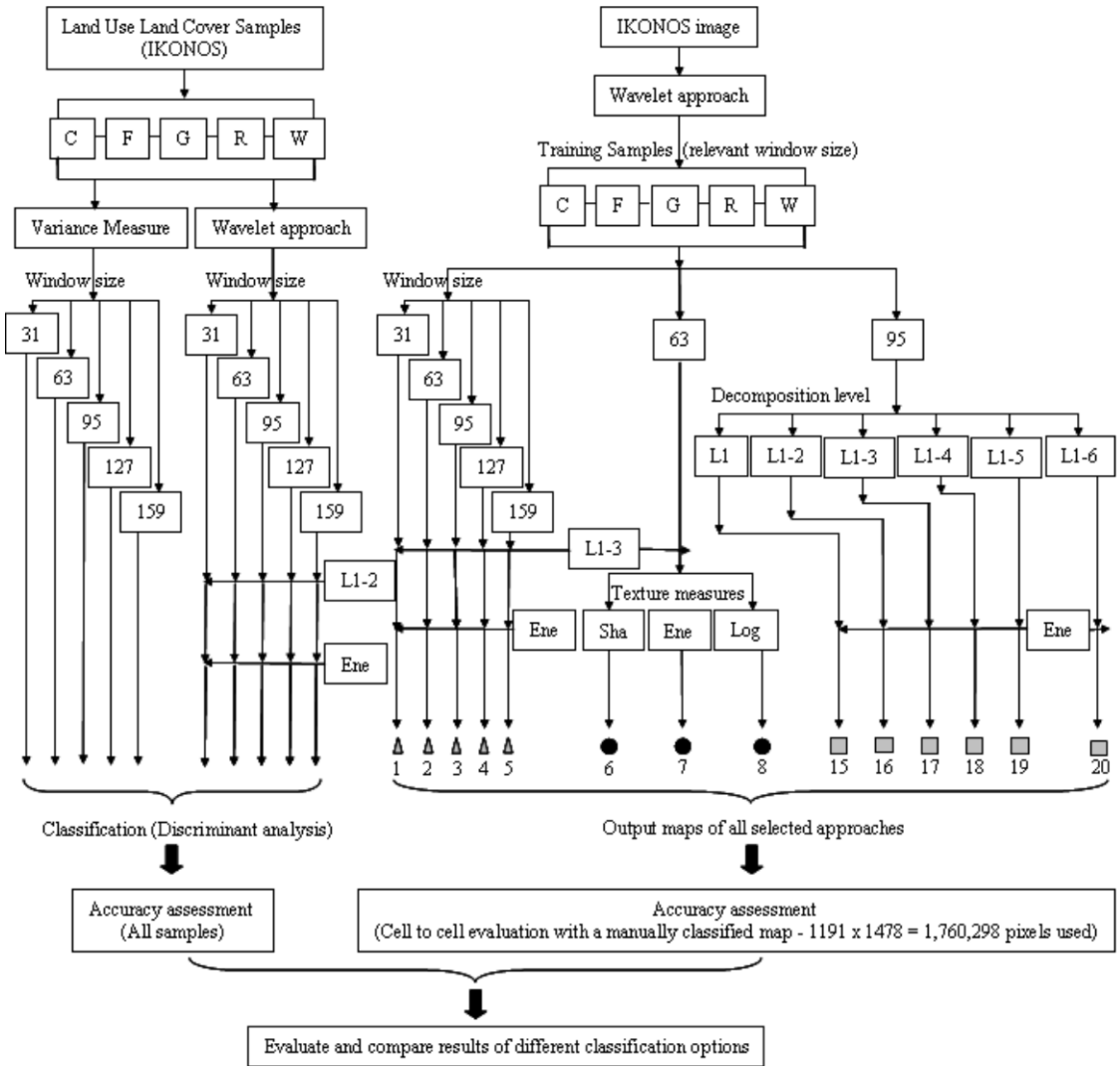

Figure 6. Research design. Note: Sha = Shannon's index; Ene = energy; Log = log energy; C = commercial; F = forest; G = grassland; R = residential; W = water; Output 1 to 5 = evaluation of window sizes; Output 6 to 8 = evaluation of texture measures; Output 15 to 20 = evaluation of scale levels.

Table 2. Overall, producer's, and user's accuracies of different window sizes of samples (i.e., 31x31, 63x63, 95x95, 127x127, 159x159) using variance measure and a discriminant function. Note: C = commercial; F = forest; G = grassland; R = residential; W = water.

	Land Use Land Cover				
	C	F	G	R	W
31x31					
Producer's Acc	27.00%	0.00%	0.00%	0.00%	23.00%
User's Acc	60.00%	0.00%	0.00%	0.00%	60.00%
	Overall Acc =	24.00%		Kappa =	0.05
63x63					
Producer's Acc	0.00%	22.00%	0.00%	0.00%	30.00%
User's Acc	0.00%	40.00%	0.00%	0.00%	60.00%
	Overall Acc =	20.00%		Kappa =	0.01
95x95					
Producer's Acc	56.00%	0.00%	100.00%	75.00%	60.00%
User's Acc	100.00%	0.00%	20.00%	60.00%	60.00%
	Overall Acc =	48.00%		Kappa =	0.35
127x127					
Producer's Acc	22.00%	0.00%	50.00%	0.00%	33.00%
User's Acc	40.00%	0.00%	20.00%	0.00%	60.00%
	Overall Acc =	24.00%		Kappa =	0.05
159x159					
Producer's Acc	50.00%	0.00%	20.00%	60.00%	50.00%
User's Acc	60.00%	0.00%	20.00%	60.00%	50.00%
	Overall Acc =	40.00%		Kappa =	0.25

Table 3. Overall, producer's, and user's accuracies of different window sizes of samples (i.e., 31x31, 63x63, 95x95, 127x127, 159x159) using energy measure of wavelet sub-images at 2 levels and a discriminant function. Note: C = commercial; F = forest; G = grassland; R = residential; W = water.

	Land Use Land Cover				
	C	F	G	R	W
31x31					
Producer's Acc	75.00%	80.00%	57.00%	80.00%	100.00%
User's Acc	60.00%	80.00%	80.00%	80.00%	80.00%
	Overall Acc =	76.00%		Kappa =	0.70
63x63					
Producer's Acc	100.00%	100.00%	80.00%	83.00%	83.00%
User's Acc	80.00%	80.00%	80.00%	100.00%	100.00%
	Overall Acc =	88.00%		Kappa =	0.85
95x95					
Producer's Acc	100.00%	100.00%	80.00%	71.00%	100.00%
User's Acc	80.00%	80.00%	80.00%	100.00%	100.00%
	Overall Acc =	88.00%		Kappa =	0.85
127x127					
Producer's Acc	100.00%	83.00%	100.00%	100.00%	100.00%
User's Acc	100.00%	100.00%	80.00%	100.00%	100.00%
	Overall Acc =	96.00%		Kappa =	0.95
159x159					
Producer's Acc	100.00%	100.00%	100.00%	100.00%	100.00%
User's Acc	100.00%	100.00%	100.00%	100.00%	100.00%
	Overall Acc =	100.00%		Kappa =	1.00

Table 4. Overall, producer's, and user's accuracies of different texture measures using 63x63 window with a combination of level 1 to 3. Note: C = commercial; F = forest; G = grassland; R = residential; W = water.

	Land Use Land Cover				
	C	F	G	R	W
Sha					
Producer's Acc	52.19%	84.79%	73.75%	4.35%	99.39%
User's Acc	65.61%	47.51%	14.58%	25.95%	73.35%
	Overall Acc =	30.17%		Kappa =	0.17
Ene					
Producer's Acc	73.05%	94.70%	34.93%	89.98%	95.59%
User's Acc	96.29%	62.51%	80.63%	82.80%	100.00%
	Overall Acc =	81.84%		Kappa =	0.68
Log					
Producer's Acc	22.99%	65.56%	36.55%	96.17%	90.37%
User's Acc	50.63%	78.56%	87.61%	75.16%	100.00%
	Overall Acc =	74.94%		Kappa =	0.50

Table 5. Overall, producer's, and user's accuracies of different window sizes (i.e., 31x31, 63x63, 95x95, 127x127, 159x159) using energy measure and a combination of level 1 to 3. Note: C = commercial; F = forest; G = grassland; R = residential; W = water.

	Land Use Land Cover				
	C	F	G	R	W
31x31					
Producer's Acc	79.29%	89.87%	45.13%	74.92%	97.76%
User's Acc	80.81%	46.18%	58.99%	83.53%	96.80%
	Overall Acc =	74.43%		Kappa =	0.59
63x63					
Producer's Acc	73.05%	94.70%	34.93%	89.98%	95.59%
User's Acc	96.29%	62.51%	80.63%	82.80%	100.00%
	Overall Acc =	81.84%		Kappa =	0.68
95x95					
Producer's Acc	45.45%	67.40%	48.81%	93.09%	92.35%
User's Acc	93.86%	92.55%	46.03%	79.58%	100.00%
	Overall Acc =	78.19%		Kappa =	0.60
127x127					
Producer's Acc	31.16%	60.05%	45.42%	96.18%	89.73%
User's Acc	93.09%	95.41%	59.21%	75.18%	100.00%
	Overall Acc =	76.66%		Kappa =	0.54
159x159					
Producer's Acc	20.67%	65.61%	35.33%	96.03%	89.03%
User's Acc	97.36%	96.40%	34.14%	76.57%	100.00%
	Overall Acc =	74.32%		Kappa =	0.50

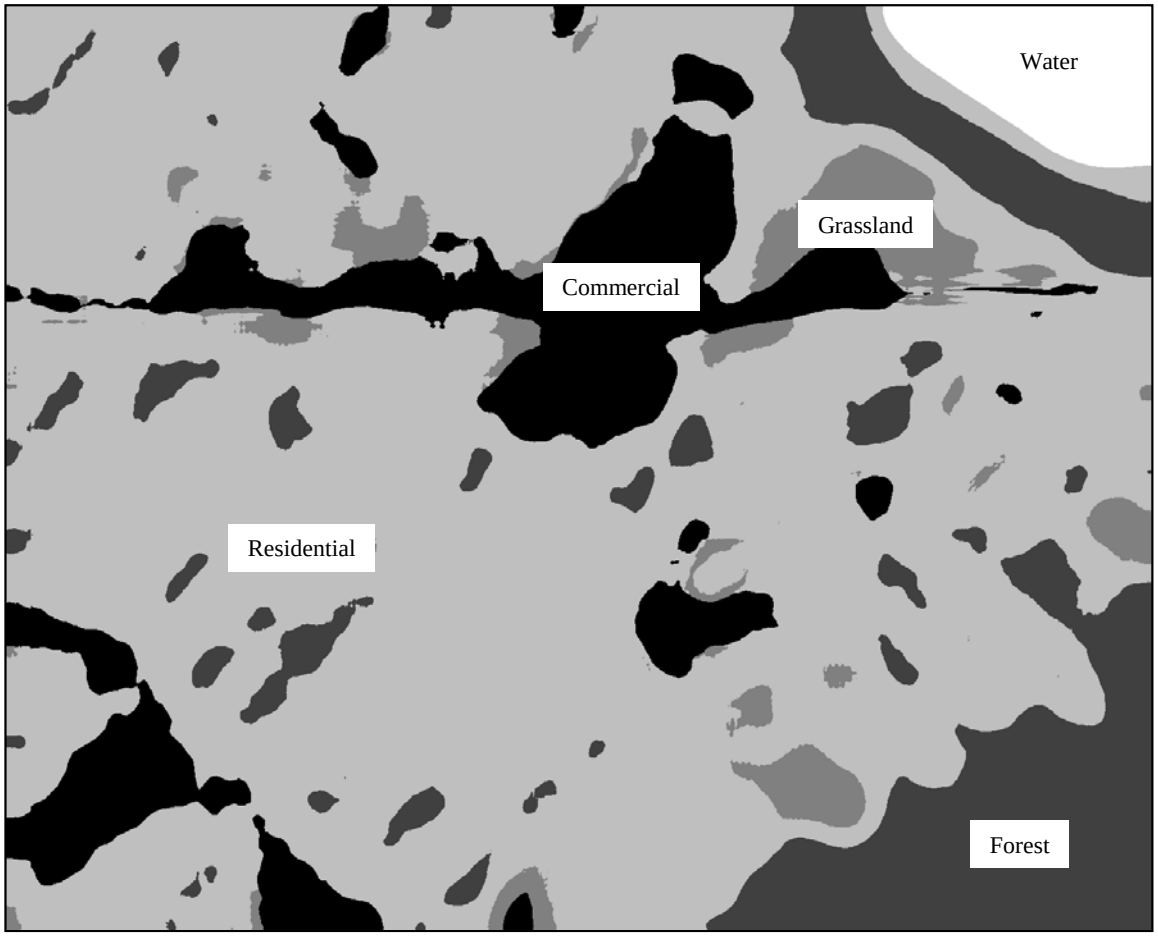

Figure 7. Classified map generated by energy measure using 63x63 window size with a combination of level 1 to 3.

Table 6. Overall, producer's, and user's accuracies of different scale level of decompositions (i.e., L1, L1-2, L1-3, L1-4, L1-5, L1-6) using energy measure and 95x95 window size. Note: C = commercial; F = forest; G = grassland; R = residential; W = water.

	Land Use Land Cover				
	C	F	G	R	W
L1					
Producer's Acc	44.72%	66.86%	49.84%	90.55%	92.26%
User's Acc	94.29%	93.05%	39.62%	79.59%	100.00%
	Overall Acc =	76.61%		Kappa =	0.57
L1-2					
Producer's Acc	45.08%	66.99%	49.42%	91.80%	92.30%
User's Acc	94.09%	92.87%	42.47%	79.60%	100.00%
	Overall Acc =	77.39%		Kappa =	0.68
L1-3					
Producer's Acc	45.45%	67.40%	48.81%	93.09%	92.35%
User's Acc	93.86%	92.55%	46.03%	79.58%	100.00%
	Overall Acc =	78.19%		Kappa =	0.60
L1-4					
Producer's Acc	45.41%	67.49%	47.87%	94.40%	92.26%
User's Acc	93.41%	92.53%	50.34%	79.38%	100.00%
	Overall Acc =	78.89%		Kappa =	0.60
L1-5					
Producer's Acc	45.93%	69.22%	47.81%	92.15%	91.94%
User's Acc	93.20%	91.87%	43.87%	79.55%	100.00%
	Overall Acc =	77.76%		Kappa =	0.59
L1-6					
Producer's Acc	43.11%	73.85%	49.92%	87.48%	88.50%
User's Acc	90.49%	89.34%	36.94%	79.19%	100.00%
	Overall Acc =	75.06%		Kappa =	0.55